

WACHEL'S EQUATION— ORIGIN AND CURRENT EVALUATION OF API 617 ROTOR STABILITY CRITERIA

by

B. Fred Evans

Rotating Equipment Specialist

Air Energi

Houston, Texas

and

John W. Fulton

Senior Engineering Advisor, Machinery

Essex Consulting Group

Gillette, New Jersey



B. Fred Evans is a Rotating Machinery Consultant for Air Energi, in Houston, Texas. He is responsible for providing machinery engineering services to various ongoing upstream projects for ExxonMobil. Mr. Evans previously worked for Shell Global Solutions after retiring from BP. Prior to joining BP (Amoco), he worked for Southwest Research Institute, providing field technical services on dynamics

problems for all areas of the energy industry.

Mr. Evans received BSME and MSME degrees from Texas Tech University (1974), and is a registered Professional Engineer in the State of Texas.



John W. Fulton retired as a Senior Engineering Advisor from ExxonMobil Research and Engineering Co. after 37 years of service. He now consults through Essex Consulting Group of Gillette, New Jersey, for ExxonMobil on rotating machinery and novel process equipment. He is co-inventor of six U.S. Patents. Mr. Fulton has presented five lectures to the Turbomachinery Symposium and three other papers to learned societies covering subsynchronous instability, rotating stall, magnetic bearings, honeycomb labyrinths, and high pressure compressors, including sour gas injection.

Mr. Fulton has a B.S. degree (Mechanical Engineering) from New Jersey Institute of Technology.

derived from an empirical equation first published by Wachel and von Nimitz (1981.) This paper discusses the origins of Wachel's Equation and illustrates by example the relationship between the two API criteria. The need to consider additional distinctions between rotors intended for different services when screening for Level 1 acceptance is shown.

INTRODUCTION

Fluid induced, aerodynamic forces exerted on a centrifugal compressor rotor within surrounding clearance spaces can be destabilizing causing nonsynchronous vibrations that may or may not become unbounded until contact between the rotor and stationary casing components occurs. Analytically, these forces are estimated by the product of the rotor's vibratory excursion and an assumed aerodynamic fluid spring, Q_{aero} , referred to as a Cross coupling stiffness having dimensions of force per unit length. Refer to APPENDIX 1 for a derivation of Q_{aero} for a circular centered orbit. This is employed as an input to a damped rotor stability analysis code such as described in Lund (1974.) A destabilizing nonsynchronous force can be exerted in a perpendicular direction to lateral shaft displacement thus coupling equations of motion in two orthogonal planes. For compressor stability screening in the design stage, the requirements of API 617 (2002) section 2.6.5 compare the subject rotor to two criteria. The first is the relationship between the ratio of Q_0/Q_A and logarithmic decrement (log dec).

- Q_0 = Applied cross coupling stiffness to yield zero log decrement
- Q_A = Anticipated cross coupling stiffness
- δ_A = Logarithmic decrement resulting from Q_A

If Q_0/Q_A is less than 2.0 or if δ_A is less than 0.1, further analyses are required.

The second criterion is the relationship between critical speed ratio (CSR) and average gas density (ρ_{AVE}). Two regions (A and B) are defined on a stability map where Level 1 or Level 2 analyses techniques are prescribed. If $2.0 < Q_0/Q_A < 10.0$ and CSR is in Region B of API 617 (2002) Figure 1.2-5, further analyses are required. Region B represents an area where centrifugal compressor stability problems have been previously experienced.

The prescribed cross coupling stiffness calculation employed to evaluate Q_A in these relationships is derived from an empirical equation first published by Wachel and von Nimitz (1981). Below are presented some of the considerations behind the Wachel formulation. These show that the Wachel formulation includes all destabilizing forces from labyrinths and impeller aerodynamic forces implied in Wachel's derivation. A series of industrial design

ABSTRACT

To satisfy API Standard 617 (2002) stability requirements, the design of centrifugal compressors must be analyzed against the Level 1 screening criteria for self-excited subsynchronous instability of the rotor lateral motion. Two criteria are given. The first compares a measure of anticipated excitation to the excitation required to predict a zero logarithmic decrement. The second compares the subject machine to a historically developed demarcation between successful and proven problematic machines. Failure to satisfy either of these two criteria requires further stability investigations be performed according to a Level 2 analysis. The two Level 1 criteria can be shown to be related. The prescribed excitation calculation employed for a Level 1 analysis has been

compressors is used as a basis to plot the first screening criterion on the coordinates of the second. This comparison shows that the two give generally similar results.

BACKGROUND

In 1980, J. C. “Buddy” Wachel created a modified form of Alford’s equation relating to Alford’s work on axial turbine stages (Alford, 1965). Its intent was to estimate input values for destabilizing force coefficients for use in rotordynamic prediction computer codes. During this rotordynamic pioneering time, stability calculations were driven forward by the prior impetus of the less than well-explained Kaybob compressor stability field results (Smith, 1975; Godard, 1973; Fowlie and Miles, 1975) and the Ekofisk gas injection compressor, vibration induced, operating limitations (Wachel, 1975; Wachel, 1982; Geary, et al., 1976). Subsequently, the empirical equation published by Wachel and von Nimitz (1981) has been extensively employed by analysts, and modified to better-fit measured test data. In one of its modified forms, it has become part of the basis for Level 1 stability screening in API 617 (2002) and as discussed in API 684 (2005). Understanding the historical development of Wachel’s Equation and its intended implementation can assist a rotordynamic analyst’s application of the API stability screening criteria. A Level 1 analysis implements only one destabilizing input (other than rotor and bearings) and it is derived from Wachel’s Equation. A compressor that fails to satisfy the Level 1 criteria must be analyzed according to Level 2 methods, which are beyond the scope of this paper.

SETTING THE STAGE

Historically, rotordynamic stability has been (and continues to be) a subject of great discussion and interest in the rotating machinery industry. In this forum and context, the manifested shaft lateral vibration associated with instability has become synonymous with project delay and increased cost. In the collective proceedings of The Turbomachinery Symposium there are quite a number of published papers dealing with the subject. Detailed case histories of stability problems should be required reading for any student that is progressing up the rotordynamic learning curve. Sometimes these case histories appear more well documented when the stability phenomenon is less well understood at the time of problem resolution and report writing. Later, as an analyst reflects on past experiences, a broader view can be developed. This was the situation when Wachel proposed his formulation and put it forward for others to examine, review and use. What has become commonly referred to as *Wachel’s Equation* and its interpretation has taken on a life of its own even though it does not always carry Wachel’s name with it.

During the 1970s, two gas reinjection centrifugal compressor stability problems received considerable attention and excellent publications exist documenting the measurements and the sequential modifications employed to achieve successful operation. These have been referred to as *Kaybob* and *Ekofisk* and the reader is encouraged to examine the references to these case histories. A particularly enlightening review can be found in chapter 7 of Vance, et al. (2010). Both of these landmark events were characterized by severe vibration as the compressors were being commissioned in the field. The unplanned, extended project completion time and increased costs to diagnose, modify, test and resolve these compressor stability problems were significant. Many modifications were tried before final successful operation was achieved at or near design conditions. Some of these attempted modifications correctly attacked certain types of destabilizing phenomena, but it was only after implementation and retest that it was discovered that the root of the problem was an additional or different, previously unrecognized, source of destabilizing forces. Other case history publications exist with descriptions of centrifugal compressor stability problems found

once a machine was tested or installed in the field and commissioned (Wachel, 1975; Wachel, 1982; Fulton, 1984b; Evans and Smalley, 1984; Smith and Wachel, 1984). One common thread was the multiphenomenon, *shot gun* approach that was applied to extinguish the problems. As destabilizing forces became better understood and new analytical methods were developed into useable stability prediction computer codes, dominant effects could be separated and addressed more easily. However, during the *early days* of reinjection stability problems, screening criteria were needed to assess a rotor’s susceptibility to destabilizing forces. This screening criteria requirement is still in place today and is fulfilled by application of equation 1.2-7 of API 617 (2002), which is an arbitrated descendent of Wachel’s original formulation.

It is interesting to note Wachel’s background and the environment in which he worked when the formulation mentioned above was created. Wachel had worked extensively with vibrations in reciprocating machinery for the natural gas transmission industry and possessed an excellent understanding of the mechanical and fluid driving forces associated with their problems and failures. At the time, many centrifugal compressor vibration analysts had a sufficient mechanical background, but lacked a good grounding in fluid thermodynamics and the interactions of fluid flow within internal machinery passages and connected piping. Wachel’s reciprocating background learnings helped transcend this gap. There were at least 10 vibration analysts working with him in a group dedicated to identifying and solving many types of existing machinery vibration problems in field settings. Additional support was readily available from mathematical and other academic resources. It was unprecedented in the industry at that time to have such a large group so well equipped to measure, model and interpret machinery vibrations. While not all phenomena were understood then and still may not be today, there existed a cultural environment conducive to progress. The inhabitants of this *Fertile Crescent* were presented with the need to resolve real time problems, had the collective necessary mechanical and fluid dynamic background, and were supplied with the best state-of-the-art modeling and measurement tools available. All this was financially supported by several industries with intolerable risk exposure once a machinery problem surfaced. One lasting testament of this confluence and resulting *perfect storm* has proven to be the basic formulation of Wachel’s Equation when used as a screening tool.

BASIS OF THE WACHEL FORMULATION

In 1980, Wachel reviewed several independent, compressor stability case histories from the prior decade trying to find a common relationship involving operating conditions, hardware dimensions, and assumed destabilizing rotor forces. Some analysts had begun applying Alford’s work related to stability of axial compressors and turbines to centrifugal machines (Kirk and Donald, 1983). Alford (1965) stated in the introduction to his paper:

“This paper considers two kinds of disturbing forces, both of aerodynamic origin. One is due to a circumferential variation of static pressure acting on the cylindrical surface of rotor, particularly within labyrinth seals. Another exciting force is due to eccentricity of rotor causing circumferential variation of blade tip clearance. There results a corresponding variation of local efficiency and unbalanced torque.”

Wachel’s intent may have been to attack the second item Alford mentioned, but time has shown his equation is now accepted for use in accounting for all aerodynamic destabilizing forces in a Level 1 analysis. Wachel began with Equation 51 from the appendix of Alford (1965), which was intended for axial flow turbine or compressor stages and he interpreted it as Equation (1) below:

$$Q_{ALFORD} = \beta * \left(\frac{T}{2 * r * h} \right) \quad (1)$$

where:

Q_{ALFORD} = Tip clearance aerodynamic loading, lbf/in
 β = Efficiency factor, usually 1 or 2
 T = Torque, in lb
 r = Blade mean radius, in
 h = Blade height, in

Wachel referred to Equation (1) as a *tip clearance equation* and adapted it to address *aerodynamic cross coupling* in centrifugal compressors. In common conversation Wachel's version was sometimes called a tip clearance effect equation for centrifugal compressors. Wachel assumed this influence for centrifugal compressors was of a similar form as that discussed by Alford (1965) for axial flow stage blade tips.

Initially, when the above equation was applied to centrifugal compressors, the results were deemed to yield too low a cross coupling stiffness value that did not correlate well with field experience. Computer codes based upon Lund's method (Lund, 1974) could be used to determine a cross coupled stiffness value that would give a log dec of zero if sufficient other input values were available. By empirically back calculating various combinations of parameters similar to those in Alford's equation and using the knowledge from published or recorded case histories that gas density played a role, the form of the equation for centrifugal compressors began to take shape. Thus the ratio of discharge density divided by suction density was introduced. However, a scaling factor was still required to create an equality between the known Q_{aero} to give a calculated zero log dec and the other parameters in the equation. Wachel suspected that this scale factor was on the order of magnitude of two.

When well head produced gas is reinjected to maintain reservoir pressure, it is usually not completely processed and contains some higher hydrocarbon species (C6+) and contaminants that would be removed or at least reduced in content as compared to pipeline quality gas. Thus the molecular weight can be on the order of 20 to 30 for these applications compared to 16 to 18 for pipeline gas. Several of the reviewed case histories involved natural gas reinjection, thus Wachel settled on using the molecular weight of the gas divided by 10 as a scaling factor. This yielded an adjustable scale factor with a value between two and three. (One can imagine that determining a scale factor in this manner could have been a similar experience to when the first determination of the Universal Gas Constant was attempted).

Figure 1 is a photocopy from one of the authors' files, showing the original form of Wachel's Equation as documented when he and Wachel worked for the same employer.

$$Q = \frac{63000 \text{ (HP)} \cdot MW \cdot P_D \cdot T_S \cdot Z_S}{D \cdot h \cdot N \cdot P_S \cdot T_D \cdot Z_D} \cdot \frac{1}{10} \quad (3)$$

Figure 1. Original Formulation of Wachel's Equation.

Thus Wachel's Equation (2) was first formulated as:

$$Q = \left(\frac{MW}{10} \right) * \left(\frac{63000 * HP}{N} \right) * \left(\frac{1}{D * h} \right) * \left(\frac{\rho_d}{\rho_s} \right) \quad (2)$$

where:

Q = Destabilizing aerodynamic cross coupling stiffness, lbf/in
 MW = Molecular weight of the gas being compressed, lb/lb mol
 HP = Compressor horsepower, hp
 N = Rotor speed, rpm
 D = Impeller diameter, in
 h = Most restrictive dimension in flow path, in
 ρ_d = Final fluid density, lb/ft³
 ρ_s = Suction fluid density, lb/ft³
 63000 = Unit conversion factor = (Torque*rpm)/horsepower

Wachel applied this equation to his reviewed case histories and found reasonable results. Application of an *aerodynamically induced* cross coupled stiffness of a magnitude calculated from this original formulation of Wachel's Equation was sufficient to drive the respective subject case history rotors to essentially a zero log dec. Based on this original formulation, the calculated cross coupling was applied to a rotor and bearing model in a damped frequency stability computer code. Compressor end casing oil seal effects were added separately in the analysis using methods such as described in Kirk and Miller (1979).

By the time the first official publication of Equation (2) appeared (Wachel and von Nimitz, 1981), the constants had been combined and rotor speed was applied in cycles per second rather than revolutions per minute as shown in Equation (3).

$$K_{xy} = \frac{B * M * P * \rho_D}{D * h * f * \rho_S} \quad (3)$$

where:

K_{XY} = Aerodynamic cross coupling, lbf/in
 B = Cross-coupling constant, 105
 M = Molecular weight of gas, lb/lb mol
 P = Power, hp
 D = Impeller diameter, in
 h = Restrictive dimension in flow path, in
 f = Speed, Hz
 ρ_D = Fluid discharge density, lbm/ft³
 ρ_S = Fluid suction density, lbm/ft³

The resulting K_{xy} (actually Q_{aero} , as the damping force, C_{xx} was not known) for a beam style compressor was applied at rotor mid span where the largest vibration deflection existed for the first forward mode shape, which is usually the mode excited in compressor stability problems. An analyst could determine the cross coupling required to yield a zero log dec and compare it to the value from Wachel's Equation. A safety factor could be deduced based on the relative position of what was now being called the *Wachel Number* to the zero log dec cross coupling on a plot of log dec as a function of cross coupling applied to a rotor. API 617 (2002) still uses this comparison in the Level 1 screening criteria. However, there have been some modifications to the Wachel Equation formulation.

Over the ensuing years since its first publication, several modifications to Wachel's Equation have been implemented by compressor manufacturers to fit their experience and by consultants/analysts to account for various specific conditions. Some of the more notable are:

- Memmott (2000) and Memmott (2002) calculated the cross coupled stiffness on a per impeller basis and applied a modal factor to account for the fact that not all rotor locations where destabilizing forces occur have the maximum vibration deflection as seen at midspan.

- Smalley analyzed a propane compressor with side streams (Smalley, et al., 2006). The method combines cross-coupling values contributed to each impeller by the side streams that flow through that impeller. It treats each stream as a separate *virtual* compressor and, in the Wachel Equation, inserts density values at that stream's points of introduction (stream suction) and discharge. Smalley obtains an impeller cross-coupling contribution by using a power value in the Wachel Equation that equals unit power multiplied by the ratio of stream mass flow to total mass flow through the impeller.

- Others used Wachel's Equation to calculate stiffness, reduce it by some percentage, and then added separately calculated values for items such as labyrinth seals (Li, et al., 2005).

These changes, in essence, modified Wachel's empirical fudge factor (mol weight/10) to fit the analyst's needs and desires based on his or her interpretation and ideas about what was actually happening inside a compressor. Some further background discussion and comment on these issues can be found in API 684 (2005).

API 617 IMPLEMENTATION

In modified form, Wachel's Equation forms part of the basis for Level 1 stability screening in the API 617 (2002) standard as the anticipated cross coupling shown in Equation (4):

$$Q_A = \sum_{i=1}^S q_{A_i} \quad (4)$$

$$q_{A_i} = \frac{HP * B_C * C * \rho_d}{D_C * H_C * N * \rho_s} \quad (5)$$

where:

- Q_A = Anticipated cross coupling for the rotor, Klbf/in
- q_{A_i} = Cross coupling defined in Equation (5) for each impeller, Klbf/in
- S = Number of impellers
- HP = Rated horsepower per impeller, hp
- B_C = 3
- C = 63
- D_C = Impeller diameter, in
- H_C = Minimum of impeller or diffuser width per impeller, in
- N = Operating speed, rpm
- ρ_d = Discharge gas density per impeller, lbm/ft³
- ρ_s = Suction gas density per impeller, lbm/ft³

The API formula is applied wheel-by-wheel, instead of flange-to-flange as in the original Wachel formulation. The other difference is that Wachel included the molecular weight, and did not include the empirical factor B_C , which is constant. Although the original formulation was derived from experience with high pressure injection machines, it is now applied to all centrifugal and axial compressors by the API standard. The API standard applies a slightly different equation for axial stages.

BASIS OF FIGURE 1.2-5 OF API 617

Sood (1979) introduced a stability map using the coordinates of rotor flexibility ratio (*spin/rigid*) versus the gas density. The density is calculated as the mean between the suction and discharge flanges. Although Sood gave no numerical values, a line was drawn to show the threshold where increasing flexibility and increasing density caused instability. Fulton (1984a, 1984b) used the same coordinates and published Figure 2 below, which gives numerical values. (The curves in Fulton, 1984a, are the same as in Fulton, 1984b, but the designations "typical" and "worst case" are from Fulton, 1984b).

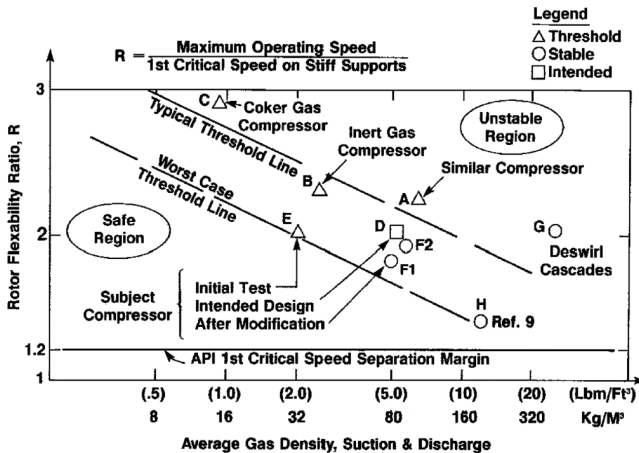


Figure 2. Fulton-Sood Stability Map.

These stability maps were based on compressors similar to those described above for gas injection duties. However, the plotted compressors were of various manufacturers' designs and had different features that affect stability, thus causing noticeable

scatter. Fulton (1984a, 1984b) did not distinguish between straight-through and back-to-back arrangements. Many types of labyrinth designs are included. Also, different tilt-pad bearing designs, placed at various distances from the nodal point of the first bending mode, introduced differing degrees of damping to the rotor system. Therefore much scatter is apparent in the empirical stability maps. Memmott (2002) plotted many more points over Figure 2 reinforcing its general trends, but without reducing the trend toward scatter.

On the Fulton (1984a, 1984b) map, all the compressors, except the inert gas compressor, had oil seals where the rotor passes through the casing. Oil seal rings can produce their own destabilizing forces, (Kirk and Miller 1979; Kirk, 1994). Recently, most injection compressors use dry gas seals, which produce negligible lateral destabilizing forces on the rotor. Thus more recent compressors are somewhat inconsistent with the stability map.

As a historical note, another version of an experience-based stability map was introduced that related a pressure parameter to critical speed ratio (Kirk and Donald, 1983; Kirk, 1985). It was used by several manufacturers; however, this map has not been addressed in the API stability criteria.

DISCUSSION OF THE TWO

API 617 LEVEL 1 CRITERIA

Alford's effect depends on tip clearance, which is directly proportional to orbit radius, which in the limit can be 100 percent of the clearance. It thus provides a feedback mechanism for instability. Wachel's assumed mechanism must depend on impeller displacement, which is not so obviously linked to a physical mechanism within the main flow passage, which could create tangential destabilizing forces on the rotor orbit.

The critical speed ratio is defined as the shaft rotational speed divided by the first bending critical speed of the rotor on rigid supports. This ratio provides a nondimensional measure of the first bending frequency, and thus of shaft stiffness, without regard to the bearing stiffness. Fulton (2003) shows the form and slope of the CSR versus density plot can be modeled by applying labyrinth forces as the sole source of destabilizing force. Labyrinth cross coupling increases with decreasing frequency, having the form shown in Equation (6).

$$Q_{aero} = K_{XY} - WRF * C_{XX} \quad (6)$$

where:

- Q_{aero} = Cross coupling due to aero forces inside labyrinth, lbf/in
- K_{XY} = Cross coupled stiffness due to aero forces inside labyrinth, lbf/in
- WRF = Whirl frequency, cycles/sec
- C_{XX} = Direct damping due to aero forces inside labyrinth, lbf sec/in

In comparison, Wachel cross-coupling is independent of any explicit frequency of the whirl orbit that occurs during subsynchronous instability. (The frequency in the Wachel formulation is the rotor spin speed). Therefore the Wachel formulation cannot properly account for labyrinth forces, even though it included them in its empirical data fit. One can expect it is only accurate for rotors where the CSR and the WFR are similar to the original data fit.

TRENDS IN ANTICIPATED CROSS-COUPLING (Q_a) BASED ON THE FORM OF THE API 617 IMPLEMENTATION

API Equation 1.2-7 (Equations 4 and 5 above) for Q_A can be recast into a form similar to Alford's original form by using the fundamental definition of torque. Refer to APPENDIX 2 for this example calculation. The result of this example is shown in Equation (7). Note that the summation over the total number of impellers is assumed in the balance of the paper.

ORIGIN AND CURRENT EVALUATION OF API 617 ROTOR STABILITY CRITERIA

$$Q_a' = \frac{B_C * Torque * \rho_d}{D_C * H_C * \rho_s} = 11817 \text{ lbf/in} \quad (7)$$

where:

- Q_a' = Cross coupling defined in Equation (7) for each impeller
- B_C = 3
- Torque = Torque on each impeller, in lbf
- D_C = Impeller diameter, in
- H_C = Minimum of impeller or diffuser width per impeller, in
- ρ_d = Discharge gas density per impeller, lbm/ft³
- ρ_s = Suction gas density per impeller, lbm/ft³

Note that this formulation of Q_a' gives the correct customary units (the same would be obtained in metric units, not shown here for brevity) without the need of any explicit adjustments with dimensional constants. The resulting Q_a' units of lbf/in represent stiffness, as expected. Note that this of course gives exactly the same numerical result. Q_a' differs from Alford's form by inclusion of the density ratio, which is of order 1. Also B_C = 3 for the API form versus 1 or 2 for Alford.

Examining Q_a' for physical significance, and neglecting the density ratio for the moment, one can see Q_a' is proportional to the ratio of torque divided by the projected area of the impeller tip. One can think of Q_a' as torque intensity. That is, Q_a' has the same numerical value for any size impeller that has the same torque per square inch of projected tip area = π × D_c × H_c. The consequence of this formulation will become apparent in the example given later in Table 1.

Note that Q_a' = Q_a is not dimensionless, thus raising the question of whether it is valid across a broad range of centrifugal compressor sizes. However, one cannot tell from the form alone if the dimensional scaling is valid, as can be seen by arguing by analogy with reciprocating internal combustion engines. Taylor (1968) points out that, for reciprocating internal combustion engines, the dimensional parameter, brake mean effective pressure (BMEP), expressed in pounds force per square inch in customary units, is constant across a large range of engine sizes, from model airplane engines up to huge ship engines, given similar construction, for instance, a two-stroke cycle without turbocharging in his example. Thus, the scaling of BMEP across a large range of sizes is satisfactory, even though it is not dimensionless. By analogy, this leaves open the question of whether Q_a scales properly.

Getting back to the density ratio, for a centrifugal compressor impeller, the density ratio is a function of tip Mach number (Ludtke, 2004). Thus Q_a becomes larger at higher tip Mach numbers, all other things remaining the same.

To better understand the physical significance and trends predicted by the API form of the anticipated cross coupling, Q_a, it is helpful to recast the equation in another form. As shown in APPENDIX 3, one can substitute the impeller flow, head, efficiency, and gas density for the power in the API form of Q_a, giving Equation (8).

$$Q_a'' = \pi * B_C * \frac{HP * V_{r_{tip}} * \rho_d * \rho_{ip}}{\eta_p * Spin * \rho_s} \quad (8)$$

where:

- π = 3.1415926
- B_C = 3
- H_p = Polytropic head per stage, ft lbf/lbm
- η_p = Polytropic efficiency per stage
- V_{r_{tip}} = Radial gas velocity at impeller tip, ft/sec
- Spin = Rotor speed, radians per second
- ρ_d = Discharge gas density per stage, lbm/ft³
- ρ_s = Suction gas density per stage, lbm/ft³
- ρ_{tip} = Impeller tip gas density per stage, lbm/ft³

Note stage refers to an impeller, diffuser, and return channel.

Consider varying the suction pressure only, while the spin, head, efficiency, flow velocities, temperature, and polytropic exponent are held constant. In this case the pressure ratio and the density ratio

do not change with suction pressure. The tip density will change. Now one can see that for the range of impellers defined above, that Q_a' is directly proportional to the gas density at the tip of the impeller. This is as expected and is consistent with Fig. 1.2-5 of API 617 (2002), which presumes that gas density is the dominant factor causing subsynchronous instability (Wagner and Steff, 1996).

EFFECT OF COMPRESSOR DESIGN ON TRENDS IN ANTICIPATED CROSS-COUPLING (Q_a) FOR A GIVEN DUTY

The spin, head, efficiency, and flow velocities are not free variables (as allowed in the above discussion) for a given compressor duty, and thus further constrain the anticipated cross-coupling, Q_a. Consider a duty where the suction pressure and temperature, discharge pressure are specified, as is the gas composition and flow rate. Allow the designer to choose one or two compressor trains to satisfy the duty. Suppose the designer compares three solutions as follows:

1. Two compressors in parallel with four impellers. This case is identical to the second stage of the eight impeller injection compressor detailed in APPENDIX 4.
2. One compressor with four larger impellers running at lower speed, with all dimensions scaled by a factor of the square root of 2. This compressor satisfies the rule of dimensional similitude, and the flow and head coefficients are identical to Case 1 (Shepherd, 1956).
3. One compressor with four impellers twice as wide as Case 1, and running at the same speed as Case 1. This compressor does not satisfy dimensional similitude, but as the tip widths are narrow in any case, the second order effects will be ignored for this discussion.

The results for the three cases are given in APPENDIX 5. Results, considering only the last impeller, and customary units for brevity, are given in Table 1.

Table 1. Scaling Defect for Alternate Duties.

(For Impeller No. 4)	units	Case 1	Case 2	Case 3
Tip diameter	Inch	18	25.45	18
Tip width	Inch	0.4	0.566	0.8
Spin	RPM	10535	7449	10535
Flow coefficient	-	0.0094	0.0094	0.0189
Head coefficient	-	0.63	0.63	0.63
Gas power	Horsepower	1785	3570	3570
Anticipated cross coupling, Q _a (API 617, Equation 1.2-7)	Lbf/in	5421	7667	5421

Note that Q_a increases by a factor of the square root of 2 comparing Case 1 to Case 2. This seems reasonable, as one expects Q_a to be larger when the duty is doubled. However, note that Q_a for Case 3 is identical to Case 1. This seems unreasonable for a doubling of the duty and a doubling of the impeller width.

From the form of Q_a' of Equation (7) above, one can see the Case 3 result is caused by the doubling of the torque being canceled by the doubling of the tip width. Thus the Case 3 result is not unexpected based on Equation (7) mathematics, but it is unexpected for a compressor with twice the power of Case 1.

METHOD OF COMPARISON OF THE TWO API CRITERIA

The comparison of the two Level 1 criteria will be anchored around a published case of subsynchronous instability on a high pressure compressor (Camatti, et al., 2003) which happens to agree well with the API version of the Modified Wachel Equation. That case is particularly interesting because it had dry gas seals and a honeycomb-versus-smooth-drum division wall seal. Both Level 1 screening criteria originated by empirically fitting cases of subsynchronous instability where the centrifugal compressors had bushing type oil seals, which are no longer common, and tooth labyrinth type internal seals. The direct

stiffness (K_{xx} or K_{yy}) was not considered for the present comparison; however if it is large it can change the whirl frequency of the rotor and needs consideration. (The direct stiffness depends heavily on any taper in the running clearance of the honeycomb).

To understand the method of comparison, consider the eight impeller compressor discussed by Camatti, et al. (2003). This rotor reached the threshold of stability on full-load test in the vendor's works at a given suction pressure and gas density. Therefore the log decrement is equal to zero at that point. Using a damped natural frequency calculation for the rotor-bearing system, the applied cross-coupled stiffness required to produce a log dec equal to zero (Q_0 in Figure 1.2-4 of API 617) can be found by iterating the applied cross-coupled stiffness against log dec in a damped natural frequency calculation. Suppose that this quantity of cross-coupling was exactly equal to the anticipated cross-coupling Q_a , calculated from the Modified Wachel Equation from API 617 (2002), for the test conditions at the stability threshold. Using the same rotor mass-elastic model, one can also calculate the critical speed ratio in Figure 1.2-5 from API 617 (2002). Using the test stand conditions, the average gas density can be also calculated.

Now one has a point $Q_a = Q_0$ for log dec = 0, for which one knows CSR and average gas density. Because it is at the threshold of stability it can be plotted on Figure 1.2-5 from API 617 (2002), which is redrawn in Figure 3.

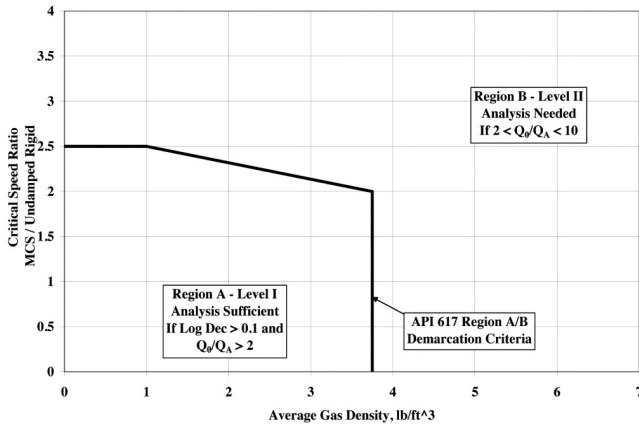


Figure 3. Level 1 Screening Criteria (API 617 [2002] Figure 1.2-5 Redrawn).

If a similar rotor were built with seven impellers, it could be run in a closed-loop test stand at a higher pressure than the rotor above, because it has a stiffer rotor. If the pressure were raised until it were unstable then another point could be calculated as above and plotted on Figure 1.2-5. The same procedure could be employed for similar compressors with any number of impellers for which the threshold of stability could be found.

CALCULATION PROCEDURE TO OVERPLOT Q_a

The above test stand procedure can be simulated by calculation to map the modified Wachel criterion onto Figure 1.2-5 of API 617 (2002).

The method of comparison starts with a set of rotor-bearing systems with varying shaft flexibility (Fulton, 2003). These rotors are similar, with the same bearings (but differing loads). The shaft diameters are also the same. The number of impellers varies from 4 to 12. This set will be formed by removing or adding stages to the discharge end of the eight impeller rotor from Camatti, et al. (2003). The speed and impeller diameter will be the same for all rotors. The cross-coupling at the threshold of instability (log decrement = 0) is calculated by a standard rotordynamics code for damped natural frequencies.

This cross coupling will be matched with the anticipated cross coupling, Q_a , calculated from the Modified Wachel Formula, by adjusting the suction pressure while holding the actual volume flow at the first impeller fixed (at its best efficiency point).

To consider compressors other than the gas injection style, a large process compressor, from an actual project, was also calculated. As before, the number of impellers was varied to give a range for plotting onto Figure 1.2-5 of API 617 (2002). This rotor is larger and heavier, and its impellers have a larger flow coefficient.

The characteristics of all the rotors used in this calculation are given in APPENDIX 4 to this paper.

RESULTS

The results of the above described calculation are illustrated in Figure 4.

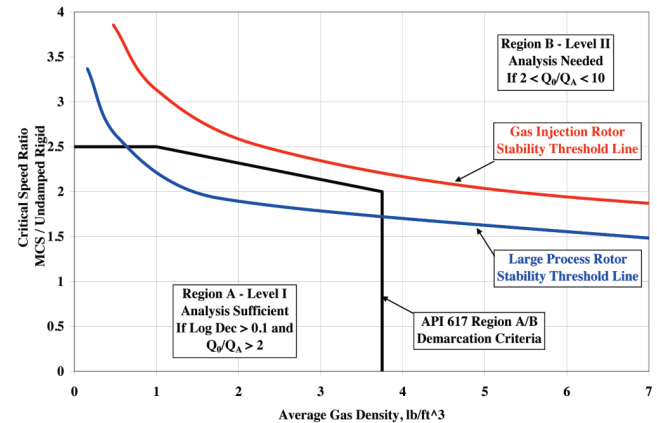


Figure 4. API 617 Stability Screening Criteria Comparison, Back-to-Back Compressor Rotors.

DISCUSSION OF THE RESULTS

The red and the blue lines in Figure 4 represent the locus of points where the log decrement is equal to zero, thus forming the stability threshold lines for the modified Wachel mapping. The threshold line for a set of large process rotors is lower than that for gas injection rotors. For a given critical speed ratio, the gas injection rotor set reaches the stability threshold at a considerably larger average gas density than the large process rotor set, and thus the injection rotors are predicted to be, by the modified Wachel mapping, the more stable of the two rotor sets.

(Note that per API 617 (2002) Level 1 criteria, a minimum log decrement of 0.1 is required, while the above mapping finds the calculated threshold of stability, where the log decrement equals zero by definition).

The modified Wachel mapping predicts the gas injection rotors are more stable than the API demarcation line (black), showing the API to be conservative as one would hope. The large process rotor is less stable than the API line, showing it does not always represent a safe design on API Figure 1.2-5, according to the modified Wachel mapping.

Figure 5 shows a semi-log plot of the information from Figure 4. This makes the slope more apparent by largely rectifying the injection and process curves. The Fulton typical line from Figure 2 above is also plotted. It crosses the Injection curve in the range of interest, but is not as steep. The slope of the Fulton line is nearly parallel to the API line, which is not surprising, given the source of the API line (Fulton, 2003). Both mappings of the Injection and Process lines are significantly steeper than the API and Fulton line. Consideration of the labyrinth Q_{aero} (Equation 6) shows that this steeper slope occurs because the Wachel formulation ignores the increased damping provided by labyrinths at the higher whirl frequencies that occur at lower critical speed ratios.

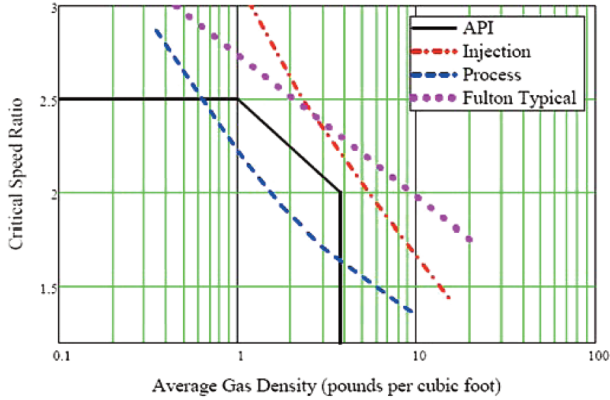


Figure 5. Stability Plot—Back-to-Back Rotors.

The large difference between the mapping of the large process versus injection and Fulton typical lines implies a large penalty against the critical speed ratio (affects bearing span and number of casings). Because Wachel made his fit using data from instability in injection compressors, and because neither the Wachel nor the modified Wachel criteria are dimensionless, (they both give lbf/in) large extrapolations of scale may not be justified. Therefore, the use of the Level 1 criteria is questionable for large process compressors.

CONCLUSIONS

- The case of subsynchronous instability on a high pressure compressor (Camatti, et al., 2003) which is featured here, agrees very well with the API version of the Modified Wachel Equation. This case is generally similar in size and construction to Kaybob and Ekofisk, but in its unstable form, has a honeycomb without shunt, and with diverging clearance in the direction of leakage flow. It has dry gas seals as opposed to Kaybob and Ekofisk. This case provides a valid basis to compare the two stability criteria in API 617 (2002). The comparison shows the two criteria in reasonable agreement, considering the empiricisms involved.

- Although Wachel's adaptation of the Alford formula implies that the source of the destabilizing forces is aerodynamic, his fitting to the empirical stability threshold did not distinguish between forces from the impeller vanes or cover, versus forces from the labyrinths. Therefore the Wachel Q_a does not represent solely an aerodynamic destabilizing effect due to the impeller vanes, but represents all destabilizing forces applied to the rotor (except possibly oil seals).

- The anticipated cross-coupling of the API form is directly proportion to gas density as expected.

- Comparing several designs for a given duty, one with double the flow, the anticipated cross-coupling calculation only gives reasonable results where the centrifugal compressor is constrained to dynamic similitude.

- By using a consistent set of industrial rotors, the applied cross coupling stiffness versus log decrement can be mapped onto the average gas density versus critical speed ratio plot by adjusting suction pressure to reach the calculated stability threshold. The position of any such curve on the map depends on the damping of the rotor bearing system, and the flow coefficient of the impellers. The damping and the flow coefficient are not considered by API 617 (2002) Figure 1.2-5.

- Mapping of the modified Wachel Equation onto the API Figure 1.2-5 does not require any assumptions about the cause of the destabilizing forces, and is based purely on Level 1 considerations.

- The use of the Level 1 criteria is questionable for large process rotors.

APPENDIX 1— DEFINITION OF Q, DERIVED FROM THE LINEARIZED FORCE MODEL

For labyrinths, the linearized force model for circular centered orbits is defined by Childs (1993) as follows:

$$\begin{pmatrix} F_x \\ F_y \end{pmatrix} = -1 \times \left[\begin{pmatrix} K & k \\ -k & K \end{pmatrix} \times \begin{pmatrix} X \\ Y \end{pmatrix} + \begin{pmatrix} C & c \\ -c & C \end{pmatrix} \times \begin{pmatrix} \dot{X} \\ \dot{Y} \end{pmatrix} \right] \quad (1-1)$$

For a circular centered orbit of radius e , the effective cross-coupled stiffness due to gas forces, Q_{aero} , can be obtained from Equation (1-1) as Equation (1-2) below. Note that $Q_{aero} > 0$ is in the same direction as the velocity of the whirl orbit, thus driving the instability.

$$Q_{aero} = \frac{F_t}{e} = k - C \times Whirl \quad (1-2)$$

where:

- C, c = Direct and cross-coupled damping coefficients
- F_t = Tangential force acting on the rotor (F)
- F_x = Force in X direction acting on the rotor (F)
- F_y = Force in Y direction acting on the rotor (F)
- K, k = Direct and cross-coupled stiffness coefficients (F/L)
- $spin$ = Rotation speed of rotor (radians/second)
- $whirl$ = Frequency of precession of the rotor around its orbit (radians/second)

APPENDIX 2— EXAMPLE OF ALTERNATE FORM OF THE API Q_a BASED ON TORQUE

Equation 1.2-7 can be recast in fully dimensioned form by writing the rotor speed, $Spin$, in units of radians per second. This eliminates the dimensional constant, $C = 9.55$ used with metric units, or $C=63$, customary units. (The factor C relates torque to rpm, and at the same time gives Q_a in thousands. Without the factor of thousands and in customary units, $C = 63025$ gives the correct dimensions for torque in inch pounds force when the $Spin$ is given in revolutions per minute and the power is given in horsepower).

$$Q_a = \frac{Power \cdot B_c}{D_c \cdot H_c \cdot Spin} \cdot \frac{\rho_d}{\rho_s} \quad (2-1)$$

For example, given:

- Power = 10000-hp
- Spin = 10000-rpm (Spin = 1047.2-rad/sec)
- D_c = 20-in
- H_c = 1-in
- B_c = 3 (a dimensionless constant that scales Q_a)
- ρ_s = 4-lb/ft³
- ρ_d = 5-lb/ft³

we find:

$$Q_a := \frac{Power \cdot B_c}{D_c \cdot H_c \cdot Spin} \cdot \frac{\rho_d}{\rho_s} = 11817 \cdot \frac{lbf}{in} \quad (2-2)$$

$$Torque := \frac{Power}{Spin} = 63025 \cdot in \cdot lbf \quad (2-3)$$

$$Q_a' := B_c \cdot \frac{Torque}{D_c \cdot H_c} \cdot \frac{\rho_d}{\rho_s} = 11817 \cdot \frac{lbf}{in} \quad (2-4)$$

APPENDIX 3—
DERIVATION OF ALTERNATE FORM
OF API Qa BASED ON IMPELLER TIP STATE

Power = $\dot{m} \cdot \Delta h$ Mass flow times enthalpy rise across the impeller internal flow
 $\dot{m} = \rho \cdot \dot{q}$ Gas density time volume flow
 $\Delta h = \frac{H_p}{\eta_p}$ Work input to internal flow is polytropic work divided by polytropic efficiency
 $\dot{q} = \text{Vel} \cdot \text{Area}$ Continuity for one dimensional flow
 $\dot{q}_{\text{tip}} = V_{r_{\text{tip}}} \cdot \text{Area}_{\text{tip}}$ Choose the impeller tip area as the flow reference for the radial velocity, $V_{r_{\text{tip}}}$
 $\text{Area}_{\text{tip}} = \pi \cdot D_c \cdot B_c$ Peripheral area of the impeller tip, using API definitions $D_c \cdot B_c$

Substituting the above:

$$\text{Power} = \dot{m} \cdot \Delta h = \rho \cdot \dot{q} \cdot \frac{H_p}{\eta_p} = \pi \cdot D_c \cdot B_c \cdot \rho_{\text{tip}} \cdot V_{r_{\text{tip}}} \cdot \frac{H_p}{\eta_p} \quad (3-1)$$

Substituting for power in the API form of Qa gives the following:

$$Qa'' = \frac{\text{Power} \cdot B_c \cdot \rho_d}{D_c \cdot H_c \cdot \text{Spin} \cdot \rho_s} = \frac{\pi \cdot D_c \cdot H_c \cdot \rho_{\text{tip}} \cdot V_{r_{\text{tip}}} \cdot \frac{H_p}{\eta_p} \cdot B_c}{D_c \cdot H_c \cdot \text{Spin}} \cdot \frac{\rho_d}{\rho_s} \quad (3-2)$$

Canceling $D_c \cdot H_c$ factors gives:

$$Qa'' = \pi \cdot B_c \cdot \frac{H_p}{\eta_p} \cdot \frac{V_{r_{\text{tip}}}}{\text{Spin}} \cdot \frac{\rho_d}{\rho_s} \cdot \rho_{\text{tip}} \quad (3-3)$$

APPENDIX 4—
TABLE OF INDUSTRIAL ROTORS
USED IN THE CALCULATION

Table 4-1.

Gas Injection Compressor Rotors - Beam Style - Two Stage - Back to Back (basis 8 Impellers)													
No of Impellers	Rotor Weight	Rotor Length	Bearing Span	Rotational Speed	No of Shaft Sections	Style	Type	Diameter	Bearings		Load 1	Load 2	Center Seal Style
									Length	Assembled Diametral Clearance			
	lb	in	in	rpm			in	in	in	in	lb	lb	
14	2641	129	109	10635	42	Tilt Pad	5 SLOP	4.7	2.0	5.5	1417	1424	Honeycomb
12	2548	118	99	10635	40	Tilt Pad	5 SLOP	4.7	2.0	5.5	1269	1279	Honeycomb
10	2256	108	89	10635	38	Tilt Pad	5 SLOP	4.7	2.0	5.5	1120	1136	Honeycomb
8	1981	97	78	10635	36	Tilt Pad	5 SLOP	4.7	2.0	5.5	971	990	Honeycomb
6	1687	87	68	10635	34	Tilt Pad	5 SLOP	4.7	2.0	5.5	822	846	Honeycomb
4	1332	75	56	10635	32	Tilt Pad	5 SLOP	4.7	2.0	5.5	662	681	Honeycomb
2	1018	67	47	10635	30	Tilt Pad	5 SLOP	4.7	2.0	5.5	495	523	Honeycomb

Large Process Compressor Rotors - Beam Style - Two Stage - Back to Back (basis 6 Impellers)													
No of Impellers	Rotor Weight	Rotor Length	Bearing Span	Rotational Speed	No of Shaft Sections	Style	Type	Diameter	Bearings		Load 1	Load 2	Center Seal Style
									Length	Assembled Diametral Clearance			
	lb	in	in	rpm			in	in	in	in	lb	lb	
10	18111	209	184	4905	80	Tilt Pad	5 SLBP	8.0	5.5	10.2	8757	9354	Laby
8	15195	183	162	4905	71	Tilt Pad	5 SLBP	8.0	5.5	10.2	7552	7634	Laby
6	12260	158	133	4905	62	Tilt Pad	5 SLBP	8.0	5.5	10.2	5994	6260	Laby
4	9335	132	107	4905	53	Tilt Pad	5 SLBP	8.0	5.5	10.2	4611	4724	Laby

Injection

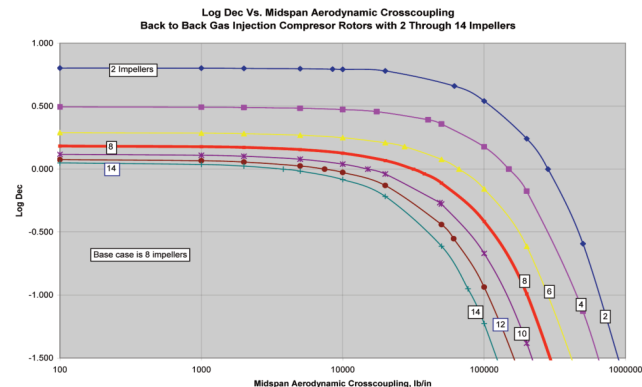


Figure 4-1.

Process

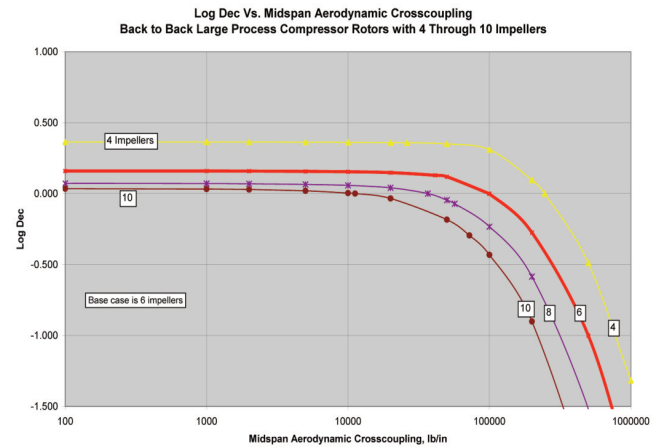


Figure 4-2.

APPENDIX 5—
CALCULATION SCALING TWO
ALTERNATE COMPRESSORS TO DOUBLE DUTY

Calculate a compressor of double the flow. Use the last four wheels of the Example Compressor, Case 1. Input data for the four wheels in flow order, from left to right as follows:

$$\text{Spin} := 10535 \cdot \text{rpm} \quad \text{Spin} = 1103.223 \frac{\text{rad}}{\text{sec}} \quad \text{case} := \text{"injection 8 wheels, 4 in stage 2"} \quad B_c = 3$$

$$\dot{w} := (1414 \ 1521 \ 1645 \ 1785)^T \cdot \text{hp}$$

$$D_{\text{tip}} := (17.000 \ 17.000 \ 18.000 \ 18.000)^T \cdot \text{in}$$

$$b_{\text{tip}} := (0.500 \ 0.500 \ 0.400 \ 0.400)^T \cdot \text{in}$$

$$\rho_d := (2.6928 \ 3.3025 \ 4.0404 \ 4.9231)^T \cdot \frac{\text{lb}}{\text{ft}^3}$$

$$\rho_s := (2.1940 \ 2.6928 \ 3.3025 \ 4.0404)^T \cdot \frac{\text{lb}}{\text{ft}^3}$$

This cross-coupling is found from the industrial code, wheel-by-wheel

$$Q_{\text{wachel}} := (3662 \ 3938 \ 5013 \ 5419)^T \cdot \frac{\text{lbf}}{\text{in}}$$

$$V_{r_{\text{tip}}} := (135.8 \ 110.7 \ 106.8 \ 87.5)^T \cdot \frac{\text{ft}}{\text{sec}}$$

$$H_p := (10612 \ 11421 \ 12345 \ 13399)^T \cdot \frac{\text{ft} \cdot \text{lb}^2}{\text{lb}}$$

$$\eta_p := (0.761 \ 0.761 \ 0.761 \ 0.761)^T$$

$$\dot{q} := (1525 \ 1242 \ 1013 \ 828)^T \cdot \frac{\text{ft}^3}{\text{min}}$$

Figure 5-1.

Find mass flow, \dot{m}_s , by continuity:

$$\dot{m}_s := \frac{\dot{q}_s \cdot \rho_s}{\eta_p} = \begin{pmatrix} 3345.9 \\ 3344.5 \\ 3345.4 \\ 3345.5 \end{pmatrix} \cdot \frac{\text{lb}}{\text{min}} \quad (5-1)$$

Calculate the flow, Φ_s , and head, μ , coefficients for the original Case 1 as follows:

$$\begin{aligned} \dot{w} &= \dot{m} \frac{H_p}{\eta_p} & \dot{m} &:= \begin{pmatrix} \dot{w} \cdot \frac{\eta_p}{H_p} \\ \dot{w} \cdot \frac{\eta_p}{H_p} \\ \dot{w} \cdot \frac{\eta_p}{H_p} \\ \dot{w} \cdot \frac{\eta_p}{H_p} \end{pmatrix} = \begin{pmatrix} 55.77 \\ 55.74 \\ 55.77 \\ 55.76 \end{pmatrix} \frac{\text{lb}}{\text{sec}} \\ U_{\text{tip}} &:= \left(\frac{D_{\text{tip}}}{2} \cdot \text{Spin} \right) = \begin{pmatrix} 781.4 \\ 781.4 \\ 827.4 \\ 827.4 \end{pmatrix} \frac{\text{ft}}{\text{sec}} & \frac{V_{r_{\text{tip}}}}{U_{\text{tip}}} &= \begin{pmatrix} 0.174 \\ 0.142 \\ 0.129 \\ 0.106 \end{pmatrix} \\ \phi_s &:= \frac{4 \dot{q} \dot{s}}{\pi \cdot U_{\text{tip}} \cdot D_{\text{tip}}^2} = \begin{pmatrix} 0.0206 \\ 0.0168 \\ 0.0115 \\ 0.0094 \end{pmatrix} & \mu &:= \frac{H_p}{U_{\text{tip}}^2} = \begin{pmatrix} 0.559 \\ 0.602 \\ 0.58 \\ 0.63 \end{pmatrix} \end{aligned}$$

Figure 5-2.

For same end states, using the above head and flow coefficients, make a double scale compressor based on the original four wheels above. The rows in the matrices represent the four impellers in flow order. The left column is the original compressor, the middle the similitude compressor, and the right the double tip width compressor, “scale” is the scaling factor, 1 for the original and $\sqrt{2}$ for the double flow machine. “s” appended to the left of the variable name indicates the scaled variables:

$$\begin{aligned} \text{scale1} &:= (1 \ \sqrt{2} \ 2) & \text{scale2} &:= (1 \ \sqrt{2} \ 1) & \text{scale3} &:= (1 \ 1 \ 2) & I &:= \begin{pmatrix} 1 \\ 1 \\ 1 \\ 1 \end{pmatrix} & JJ &:= (1 \ 1 \ 1) \\ sD_{\text{tip}} &:= D_{\text{tip}} \cdot \text{scale2} = \begin{pmatrix} 17 & 24.042 & 17 \\ 17 & 24.042 & 17 \\ 18 & 25.456 & 18 \\ 18 & 25.456 & 18 \end{pmatrix} \text{in} & sb_{\text{tip}} &:= b_{\text{tip}} \cdot \text{scale1} = \begin{pmatrix} 0.5 & 0.707 & 1 \\ 0.5 & 0.707 & 1 \\ 0.4 & 0.566 & 0.8 \\ 0.4 & 0.566 & 0.8 \end{pmatrix} \text{in} \\ \text{Keep the same flow coefficient for column 2 and double that for column 3. Keep same head coefficients:} & & & & & & & & & \\ s\phi_s &:= \phi_s \cdot \text{scale3} = \begin{pmatrix} 0.0206 & 0.0206 & 0.0413 \\ 0.0168 & 0.0168 & 0.0336 \\ 0.0115 & 0.0115 & 0.0231 \\ 0.0094 & 0.0094 & 0.0189 \end{pmatrix} & s\mu &:= \mu \cdot JJ = \begin{pmatrix} 0.559 & 0.559 & 0.559 \\ 0.602 & 0.602 & 0.602 \\ 0.58 & 0.58 & 0.58 \\ 0.63 & 0.63 & 0.63 \end{pmatrix} \end{aligned}$$

Note Spin scales inversely:

$$s\text{Spin} := I \left(\text{Spin} \cdot \frac{1}{\text{scale2}} \right) = \begin{pmatrix} 10535 & 7449 & 10535 \\ 10535 & 7449 & 10535 \\ 10535 & 7449 & 10535 \\ 10535 & 7449 & 10535 \end{pmatrix} \quad sU_{\text{tip}} := \left(\frac{sD_{\text{tip}}}{2} \cdot s\text{Spin} \right) = \begin{pmatrix} 781 & 781 & 781 \\ 781 & 781 & 781 \\ 827 & 827 & 827 \\ 827 & 827 & 827 \end{pmatrix} \frac{\text{ft}}{\text{sec}}$$

Calculate flow and head from above:

$$s\dot{q} \dot{s} := \left(s\phi_s \frac{\pi}{4} sU_{\text{tip}} \cdot sD_{\text{tip}}^2 \right) = \begin{pmatrix} 1525 & 3050 & 3050 \\ 1242 & 2484 & 2484 \\ 1013 & 2026 & 2026 \\ 828 & 1656 & 1656 \end{pmatrix} \frac{\text{ft}^3}{\text{min}}$$

Figure 5-3.

Keep same efficiency and density:

$$\begin{aligned} sH_p &:= \left(s\mu \cdot sU_{\text{tip}}^2 \right) = \begin{pmatrix} 10612 & 10612 & 10612 \\ 11421 & 11421 & 11421 \\ 12345 & 12345 & 12345 \\ 13399 & 13399 & 13399 \end{pmatrix} \frac{\text{ft} \cdot \text{lb}_f}{\text{lbm}} & s\eta_p &:= \eta_p \cdot JJ = \begin{pmatrix} 0.761 & 0.761 & 0.761 \\ 0.761 & 0.761 & 0.761 \\ 0.761 & 0.761 & 0.761 \\ 0.761 & 0.761 & 0.761 \end{pmatrix} \\ s\rho_s &:= \rho_s \cdot JJ = \begin{pmatrix} 2.194 & 2.194 & 2.194 \\ 2.693 & 2.693 & 2.693 \\ 3.303 & 3.303 & 3.303 \\ 4.04 & 4.04 & 4.04 \end{pmatrix} \frac{\text{lb}}{\text{ft}^3} & s\rho_d &:= \rho_d \cdot JJ = \begin{pmatrix} 2.693 & 2.693 & 2.693 \\ 3.303 & 3.303 & 3.303 \\ 4.04 & 4.04 & 4.04 \\ 4.923 & 4.923 & 4.923 \end{pmatrix} \frac{\text{lb}}{\text{ft}^3} \end{aligned}$$

Figure 5-4.

Calculate power:

$$s\dot{w} \dot{s} := \left(s\rho_s \cdot s\dot{q} \dot{s} \cdot \frac{sH_p}{s\eta_p} \right) = \begin{pmatrix} 1414 & 2828 & 2828 \\ 1521 & 3042 & 3042 \\ 1645 & 3289 & 3289 \\ 1785 & 3570 & 3570 \end{pmatrix} \text{hp} \quad \frac{s\dot{w} \dot{s}^{(1)}}{s\dot{w} \dot{s}^{(0)}} = \begin{pmatrix} 2 \\ 2 \\ 2 \\ 2 \end{pmatrix}$$

Figure 5-5.

Now calculate the Qwachel for the scaled set of wheels, and note that the Qa follows the scaling factor, $\sqrt{2}$ for the second column:

$$sQ_a := \left(\frac{s\dot{w} \dot{s} \cdot B_c}{sD_{\text{tip}} \cdot sb_{\text{tip}} \cdot s\text{Spin}} \cdot s\rho_d \right) = \begin{pmatrix} 3664 & 5182 & 3664 \\ 3939 & 5570 & 3939 \\ 5015 & 7093 & 5015 \\ 5421 & 7667 & 5421 \end{pmatrix} \frac{\text{lb}_f}{\text{in}} \quad \frac{sQ_a^{(1)}}{sQ_a^{(0)}} = \begin{pmatrix} 1.414 \\ 1.414 \\ 1.414 \\ 1.414 \end{pmatrix}$$

Figure 5-6.

Compare the left and the right columns. Note the Wachel result does not change with tip width, given the same diameter impeller!

REFERENCES

Alford, J. S., October 1965, “Protecting Turbomachinery from Self-Excited Rotor Whirl,” *Journal of Engineering for Power*, ASME, pp. 333-344.

API Standard 617, 2002, “Axial and Centrifugal Compressors and Expander-Compressors for Petroleum, Chemical and Gas Industry Services,” Seventh Edition, American Petroleum Institute, Washington, D.C.

API Standard 684, 2005, “Tutorial on Rotordynamics: Lateral Critical, Unbalance Response, Stability, Train Torsional and Rotor Balancing,” Second Edition, American Petroleum Institute, Washington, D.C.

Camatti, M., Vannini, G., Fulton, J., and Hopenwasser, F., 2003, “Instability of a High Pressure Compressor Equipped with Honeycomb Seals,” *Proceedings of the Thirty-Second Turbomachinery Symposium*, Turbomachinery Laboratory, Texas A&M University, College Station, Texas, pp. 39-48.

Childs, D. W., 1993, *Turbomachinery Rotordynamics, Phenomena, Modeling, and Analysis*, New York, New York: John Wiley & Sons.

Evans, B. F. and Smalley, A. J., 1984, “Subsynchronous Vibrations in a High Pressure Compressor: A Case History,” *Rotordynamic Instability Problems in High Performance Turbomachinery*, NASA Conference Publication 2338, Texas A&M University, College Station, Texas, pp. 17-36.

Fulton, J. W., 1984a, “The Decision to Full Load Test a High Pressure Centrifugal Compressor in its Module Prior to Tow-out,” IMechE Second European Congress, *Fluid Machinery for the Oil, Petrochemical and Related Industries*, The Hague, pp.133-138.

Fulton, J. W., 1984b, “Full Load Testing in the Platform Module Prior to Tow Out: A Case History of Subsynchronous Instability,” *Rotordynamic Instability Problems in High Performance Turbomachinery*, NASA Conference Publication 2338, Texas A&M University, College Station, Texas, pp. 1-16.

Fulton, J. W., 2003, “Rotor Stability Criteria for Multi-stage Centrifugal Compressors,” *Proceedings of ASME DETC’03*, Chicago, Illinois.

Fowlie, D. W. and Miles, D. D., 1975, “Vibration Problems with High Pressure Centrifugal Compressors,” ASME Paper 75-PET-28.

Geary, C. H., Damratowski, L. P., and Seyer, C., 1976, “Design and Operation of the World’s Highest Pressure Gas Injection Centrifugal Compressors,” *Journal of the Society of Petroleum Engineers*, AIME, Offshore Technology Conference, Houston, Texas, pp. 651-662.

- Godard, K. E., September 1973, "Gas Plant Startup Problems," *Hydrocarbon Processing*, pp.151-155.
- Kirk, R. G., 1985, "Evaluation of Aerodynamic Instability Mechanisms for Centrifugal Compressors," ASME Paper 85-DET-47.
- Kirk, R. G., 1994, "Analysis and Design of Floating Oil Ring Seals for Centrifugal Compressors," *Proceedings, The Fourth International Conference on Rotor Dynamics*, IFToOM, pp. 185-190.
- Kirk, R. G. and Donald, G. H., 1983, "Design Criteria for Improved Stability of Centrifugal Compressors," *Rotor Dynamical Instability*, AMD 55, American Society of Mechanical Engineers, New York, New York, pp. 59-71.
- Kirk, R. G. and Miller, W. H., 1979, "The Influence of High Pressure Oil Seals on Turbo Rotor Stability," *ASLE Transactions*, 22, (1), pp. 14-24.
- Li, J., De Choudhury, P., Sharples, M., and Wright, J., 2005, "Experiences and Applications of API 617 Full Stability Analysis (Level II) on Centrifugal Compressors," *Proceedings of the Thirty-Fourth Turbomachinery Symposium*, Turbomachinery Laboratory, Texas A&M University, College Station, Texas, pp. 35-43.
- Ludtke, K. H., 2004, *Process Centrifugal Compressors, Basics, Function, Operation, Design, Application*, Berlin, Germany: Springer-Verlag.
- Lund, J. W., May 1974, "Stability and Damped Critical Speeds of a Flexible Rotor in Fluid-Film Bearings," *Journal for Engineering in Industry*, pp. 509-517.
- Memmott, E. A., 2000, "Empirical Estimation of a Load Related Cross-Coupled Stiffness and the Lateral Stability of Centrifugal Compressors," 18th Machinery Dynamics Seminar, Canadian Machinery Vibration Association, Halifax, Nova Scotia, Canada, pp. 9-20.
- Memmott, E. A., 2002, "Lateral Rotordynamic Stability Criteria for Centrifugal Compressors," 20th Machinery Vibration Seminar, Canadian Machinery Vibration Association, Quebec City, Quebec, Canada.
- Shepherd, D. G., 1956, *Principles of Turbomachinery*, Toronto, Canada: The Macmillan Company.
- Smalley, A. J., Camatti, M., Childs, D. W., Hollingsworth, J. R., Vannini, G., and Carter, J. J., October 2006, "Dynamic Characteristics of the Diverging Taper Honeycomb-Stator Seal," *Journal of Turbomachinery*, pp. 717-724.
- Sood, V. K., 1979, "Design and Full Load Testing of a High Pressure Centrifugal Natural Gas Injection Compressor," *Proceedings of the Eighth Turbomachinery Symposium*, Turbomachinery Laboratory, Texas A&M University, College Station, Texas, pp. 35-42.
- Smith, D. R. and Wachel, J. C., 1984, "Experiences with Nonsynchronous Forced Vibration in Centrifugal Compressors," *Rotordynamic Instability Problems in High Performance Turbomachinery*, NASA Conference Publication 2338, Texas A&M University, College Station, Texas, pp. 37-52.
- Smith, K. J., 1975, "An Operation History of Fractional Frequency Whirl," *Proceedings of the Fourth Turbomachinery Symposium*, Turbomachinery Laboratory, Texas A&M University, College Station, Texas, pp. 115-125.
- Taylor, C. F., 1968. *The Internal Combustion Engine in Theory and Practice*, Volume I, Cambridge, Massachusetts: MIT Press.
- Vance, J., Zeidan, F., and Murphy, B., 2010, *Machinery Vibration and Rotordynamics*, New Jersey: John Wiley & Sons, Inc.
- Wachel, J. C., 1975, "Nonsynchronous Instability of Centrifugal Compressors," ASME Paper 75-PET-22.
- Wachel, J. C., 1982, "Rotordynamic Instability Field Problems," Second Workshop on Rotordynamic Instability of High Performance Turbomachinery, NASA Conference Publication 2250, Texas A&M University, College Station, Texas, pp. 1-20.
- Wachel, J. C. and von Nimitz, W. W., November 1981, "Ensuring the Reliability of Offshore Gas Compression Systems," *Journal of Petroleum Technology*, AIME, pp. 2252-2260.
- Wagner, N. G. and Steff, K., 1996, "Dynamic Labyrinth Coefficients from a High-Pressure Full-Scale Test Rig Using Magnetic Bearings," *Rotordynamic Instability Problems in High-Performance Turbomachinery*, NASA Conference Publication 3344, Texas A&M University, College Station, Texas, pp. 95-112.

ACKNOWLEDGEMENTS

The authors thank ExxonMobil Research & Engineering Company for permission to publish this paper.